

# Heat and Mass Transfer in a Saturated Porous Medium Confined in Cylindrical Annular Geometry

A. Ja, J. Belabid, A. Cheddadi

**Abstract**—This paper reports the numerical simulation of double-diffusive natural convection flows within a horizontal annular filled with a saturated porous medium. The analysis concerns the influence of the different parameters governing the problem, namely, the Rayleigh number  $Ra$ , the Lewis number  $Le$  and the buoyancy ratio  $N$ , on the heat and mass transfer and on the flow structure, in the case of a fixed radius ratio  $R = 2$ . The numerical model used for the discretization of the dimensionless equations governing the problem is based on the finite difference method, using the ADI scheme. The study is focused on steady-state solutions in the cooperation situation.

**Keywords**—Natural convection, double-diffusion, porous medium, annular geometry, finite differences.

## I. INTRODUCTION

THE study of heat and mass transfer within porous media has been the subject of a large number of studies in recent decades, due to its numerous applications (thermal insulation, heat exchangers...). Cavities of different geometries have been considered, such as the rectangular cavity, purely thermal [1], [2] or double diffusive [3], [4]. The vertical annular cavities subject to horizontal temperature gradients have been widely studied numerically and analytically [5], [6], constant temperature and concentration imposed across the vertical walls [7]-[9] or with opposing temperature and concentration gradients, were also studied numerically in this configuration [10]. Most of the existing works on natural convection in a horizontal annular porous media are concerned with the case of a cavity subject to temperature gradients [11]-[14], and the double-diffusive natural convection has been investigated in the presence of the Soret effect [15], [16]. In this study, we consider the double-diffusive convection in a horizontal porous annular layer, bounded by two coaxial, horizontal cylinders subjected to constant and uniform temperatures and concentrations (Fig. 1). The porous medium is saturated by a viscous binary fluid. The paper is aimed to present the effect of control parameters, namely, the thermal Rayleigh number  $0.1 \leq Ra \leq 200$ , the buoyancy ratio  $0 \leq N \leq 7$  and the Lewis number  $0.01 \leq Le \leq 60$ , on the flow structure and the thermal and solutal transfers. The radius ratio is kept constant  $R = 2$ . The Boussinesq approximation is assumed to be valid.

A. Ja and J. Belabid are with the "Thermal Systems and Real Flows", Mohammadia School of Engineers, Mohammed V University, Rabat, Morocco (e-mail: jaahmed@hotmail.fr, belabide@gmail.com).

A. Cheddadi is director of Research Team "Thermal Systems and Real Flows", Mohammadia School of Engineers, Mohammed V University, Rabat, Morocco (corresponding author, phone: +212-5-37770598; fax: +212-5-37778853; e-mail: cheddadi@emi.ac.ma).

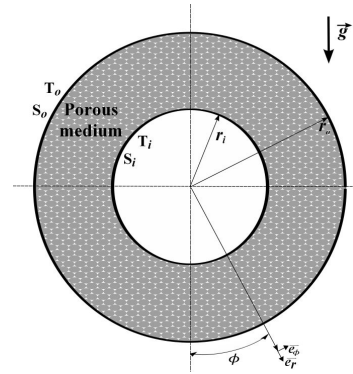


Fig. 1 Schematic of the problem under investigation

## II. PROBLEM FORMULATION AND NUMERICAL METHOD

### A. Equations

The dimensionless steady state equations governing the two-dimensional flow described in stream function formulation are given by:

$$\nabla^2 \psi = -Ra \left[ \left( \sin \varphi \frac{\partial T}{\partial r} + \frac{\cos \varphi}{r} \frac{\partial T}{\partial \varphi} \right) + N \left( \sin \varphi \frac{\partial S}{\partial r} + \frac{\cos \varphi}{r} \frac{\partial S}{\partial \varphi} \right) \right] \quad (1)$$

$$(\vec{V} \cdot \nabla) T = \nabla^2 T \quad (2)$$

$$(\vec{V} \cdot \nabla) S = Le^{-1} \nabla^2 S \quad (3)$$

where  $T$  and  $S$  are the adimensional temperature and concentration,  $\psi$  the stream function defined by  $U = \frac{1}{r} \frac{\partial \psi}{\partial \varphi}$  and  $V = -\frac{\partial \psi}{\partial r}$ , where  $U$  and  $V$  are respectively the radial and tangential velocities. In the above equations  $Ra$  is the Rayleigh number given by  $Ra = \frac{g \beta_T \Delta T r_i^3}{\nu \alpha}$ ,  $N$  the buoyancy ratio given by  $N = \frac{\beta_S \Delta S}{\beta_T \Delta T}$ ,  $Le$  the Lewis number given by  $Le = \frac{\alpha}{D}$  and  $R$  is the radius ratio defined by  $R = \frac{r_o}{r_i}$ . The heat and mass transfers are evaluated by the average Nusselt and Sherwood numbers defined respectively by  $\overline{Nu} = -\frac{1}{\pi} \ln R \int_0^\pi \frac{\partial T}{\partial r} \Big|_{r=1} d\varphi$  and  $\overline{Sh} = -\frac{1}{\pi} \ln R \int_0^\pi \frac{\partial S}{\partial r} \Big|_{r=1} d\varphi$ .

The dimensionless boundary conditions are:

$$T = 1, S = 1 \text{ and } \frac{\partial \psi}{\partial \varphi} = 0 \text{ for } r = 1, \forall \varphi \quad (4)$$

$$T = 0, S = 0 \text{ and } \frac{\partial \psi}{\partial \varphi} = 0 \text{ for } r = R, \forall \varphi \quad (5)$$

The geometric symmetry of the problem studied leads to the addition of two boundary conditions:

$$\forall \phi = 0, \pi : \frac{\partial T}{\partial \phi} = 0 \text{ and } \frac{\partial \psi}{\partial r} = 0, \forall r \quad (6)$$

### B. Numerical Method

The governing equations are discretized using a central Finite Difference method. The iterative procedure is performed with the Alternating Direction Implicit scheme (ADI). Preliminary tests conducted to examine the effect of the grid size on the obtained results showed that a 91x111 grid is sufficient. The accuracy of the numerical code was checked in the case of pure thermal convection using the results reported in [11]. The computed heat transfer rates (not shown here) are in good agreement. The iterative process is completed when the following criterion is satisfied in each node of the grid:  $\left| \frac{\chi^{n+1} - \chi^n}{\chi^n} \right| \leq 10^{-6}$ , where  $\chi$  refers to  $T$ ,  $S$  or  $\psi$ .

## III. RESULTS AND DISCUSSION

### A. Effect of Rayleigh number

In this section we are interested in the effect of Rayleigh number on the flow structure and on the heat and mass transfers, in the case of cooperating thermosolutal convection  $N = 1$ , for equal thermal and solutal diffusivities  $Le = 1$ . Figs. 2 (a)-(d), correspond to isocontours for different Rayleigh number values  $Ra = 0.1$  to 200.

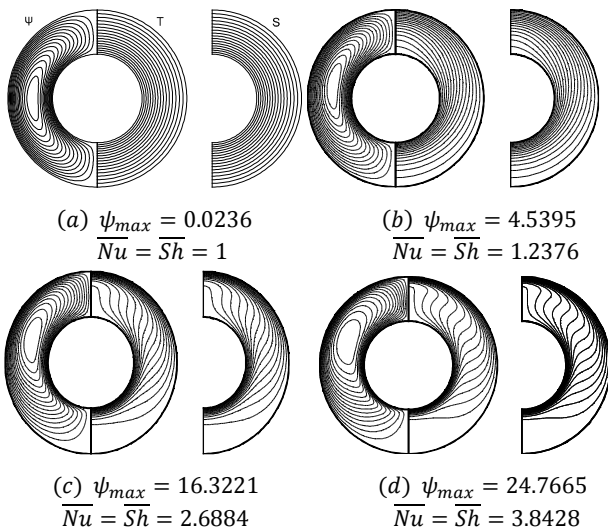


Fig. 2 Streamlines, isotherms and isoconcentrations for different values of  $Ra$  for  $N = 1$  and  $Le = 1$  (a)  $Ra = 0.1$ , (b)  $Ra = 20$ , (c)  $Ra = 100$ , (d)  $Ra = 200$

The streamlines show that the flow is unicellular clockwise in the left half-annulus. At very low values of the Rayleigh number ( $Ra \leq 1$ ), the isotherms and isoconcentrations are stratified in the radial direction, showing that the thermal and solutal transfers occur by conduction. The average Nusselt and Sherwood numbers are identical ( $Le = 1$ ) and of the order of unity. The increase of the Rayleigh number leads to an increase in the flow intensity and dynamic, thermal and solutal

boundary layers develop on the inner and outer walls. The shape of the isotherms and isoconcentrations shows a change in the mode of transfer: convective regime emerges after a state of conduction/diffusion.

The isocontours shown in Figs. 3 (a)-(d) for the same range of the Rayleigh number, with  $N = 1$  and  $Le = 5$ , shows that, for small values of the Rayleigh number ( $Ra \leq 1$ ), the results are similar to those illustrated in the case  $Le = 1$ .

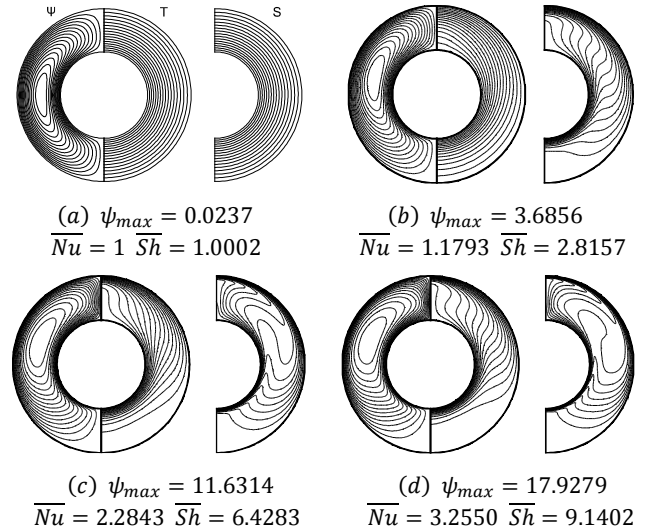
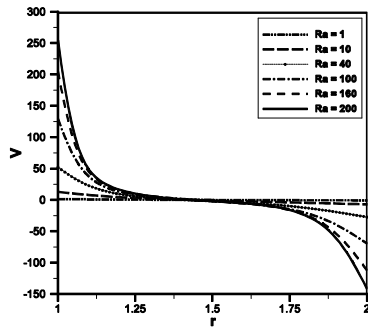


Fig. 3 Streamlines, isotherms and isoconcentrations for different values of  $Ra$  for  $N = 1$  and  $Le = 5$  (a)  $Ra = 0.1$ , (b)  $Ra = 20$ , (c)  $Ra = 100$ , (d)  $Ra = 200$

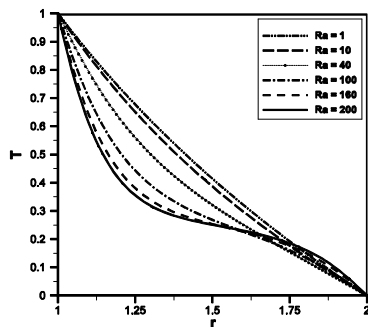
We note that the flow intensity increases with the increase of Rayleigh number, illustrated by increase in the amplitude of the tangential component of velocity close to the active walls (Fig. 4 (a)), which leads to a reduction in the thickness of the dynamic boundary layer. The comparison between the isotherms shown in the cases  $Le = 1$  and  $Le = 5$ , shows that for a same value of Rayleigh number, the isotherms are practically identical, so that the mode of heat transfer depends primarily on the Rayleigh number whereas, the isoconcentrations are strongly deformed in the core region of the cavity. Because of the great value of the Lewis number  $Le = 5$ , the form of the isoconcentrations indicates that the solutal convection is strong. The slopes of the temperature profiles (Fig. 4 (b)) and particularly concentration profiles (Fig. 4 (c)) indicate that when increasing the Rayleigh number, the thermal and solutal boundary layer regimes grow at the active walls, which clearly explains the shape of the isotherms and isoconcentrations shown in Fig. 2. Yet, the concentration in the core region of the cavity is almost equal to 0.5 for  $Ra$  values from 160 onwards.

Fig. 5 shows the evolution of the mean Nusselt and Sherwood numbers respectively for different Rayleigh numbers. For  $Ra \leq 1$ , the values of  $\overline{Nu}$  and  $\overline{Sh}$  are of the order of unity (transfer by conduction). The increase in  $Ra$ , leads to a monotonic increase in thermal and solutal transfers. Because of the high value of the Lewis number ( $Le = 5$ ), the rate of solutal transfer is more important than that of heat transfer.

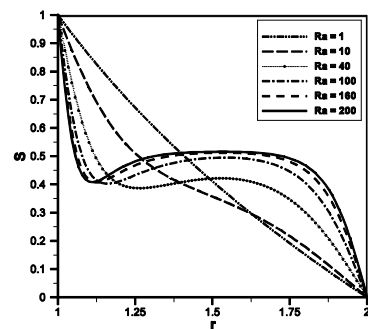
For example, we find that the solutal transfer is 282% of the thermal ones.



(a)



(b)



(c)

Fig. 4 Tangential velocity, temperature and concentration distribution for  $\phi = \frac{\pi}{2}$  for different values of  $Ra$  for  $N = 1$  and  $Le = 5$

### B. Effect of Lewis number

Fig. 6 presents the impact of the Lewis number on the flow structure and on heat and mass transfers for a range of  $Le = 0.1$  to 60 with  $Ra = 50$  and  $N = 1$ . The increase in the Lewis number causes a decrease in the flow intensity. The isoconcentrations are strongly influenced by the value of  $Le$ , their form shows that the solutal flux is increasingly convective with increasing  $Le$ . At a small Lewis number ( $Le = 0.1$ ), the solutal boundary layers are no longer distinct, and the mass transfer is mainly due to the diffusion of species. Beyond the value  $Le = 1$ , the isoconcentrations show that the solutal transfer is dominated by convection. A low solutal gradient in the core region of the cavity is distinguished and solutal boundary layers are much pronounced compared to the

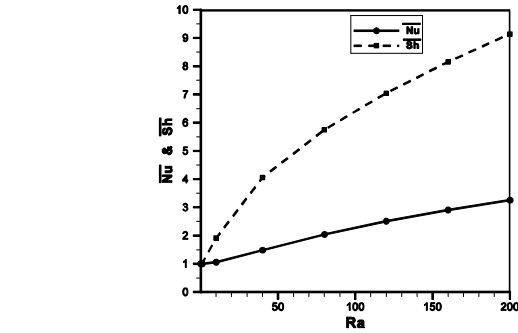


Fig. 5 Evolution of the average Nusselt and Sherwood numbers for different values of  $Ra$ , for  $N = 1$  and  $Le = 5$

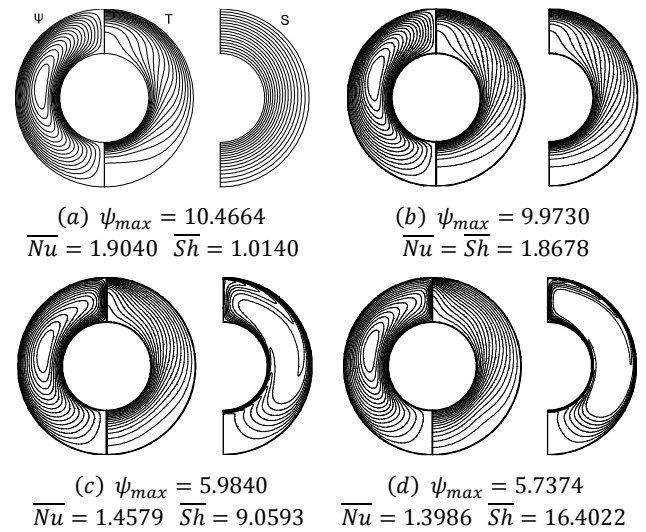
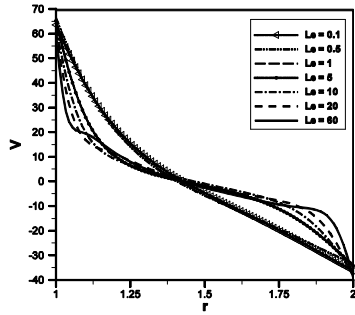


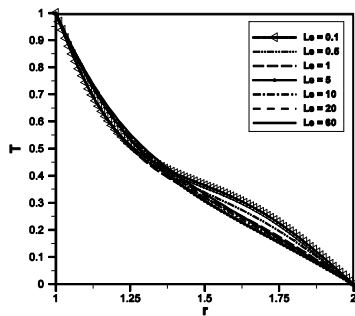
Fig. 6 Streamlines, isotherms and isoconcentrations for different values of  $Le$  for  $Ra = 50$  and  $N = 1$  (a)  $Le = 0.1$ , (b)  $Le = 1$ , (c)  $Le = 20$ , (d)  $Le = 60$

From Fig. 7, it appears that the temperature distribution characterized by low thermal gradients, since the effect of the Lewis number is negligible on heat transfer (Fig. 7 (b)). While concentration gradients near the active walls indicate that the solutal boundary layers are thinner with increasing  $Le$ , and in the center of the cavity the concentration is almost constant (Fig. 7 (c)).

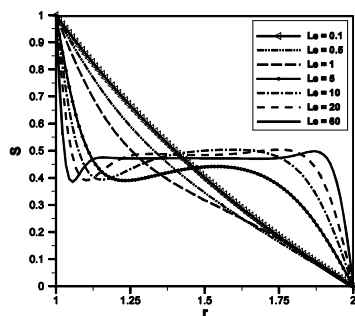
Fig. 8 illustrates the influence of the Lewis number on heat and mass transfers. The average Nusselt number decreases gradually to an asymptotic value. In contrast, the mean Sherwood number gradually increases. Note that the Sherwood number approaches unity when  $Le$  is small enough ( $\approx 0.01$ ) and the rate of thermal and solutal transfers are identical when  $Le = 1$ .



(a)



(b)



(c)

Fig. 7 Tangential velocity, temperature and concentration distribution for  $\phi = \frac{\pi}{2}$  for different values of  $Le$  for  $Ra = 50$  and  $N = 1$

C. Effect of Buoyancy Ratio

Fig. 9 illustrates the effect of the buoyancy ratio in the cooperating case  $N \geq 0$  on the flow structure. When  $N = 0$ , the resulting flow is purely thermal. For  $N \ll 1$ , the thermal buoyancy forces are dominant, while in the opposite case  $N \gg 1$ , the flow is controlled by solutal buoyancy effects. Note that, the increase of  $N$  in the cooperative cases, the thermal and the solutal buoyancy forces drive the intensified flow in the same direction. In this situation, the concentration gradients strengthen the temperature and the velocity gradients near the active walls. This trend is illustrated in Fig. 10 (a) showing increasing amplitude of the tangential component of velocity with the buoyancy ratio. Consequently, the rates of heat and mass transfers are represented in Fig. 11, increase with  $N$  under a convective regime. But because of the high  $Le$ , the average Sherwood number is more important than the Nusselt number. For example, for  $N = 5$  the solutal transfer is 321% of the thermal one.

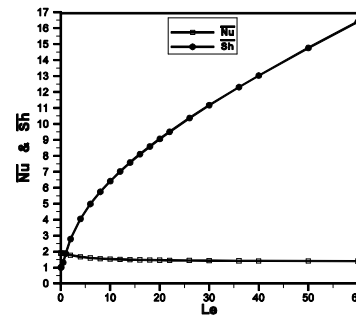
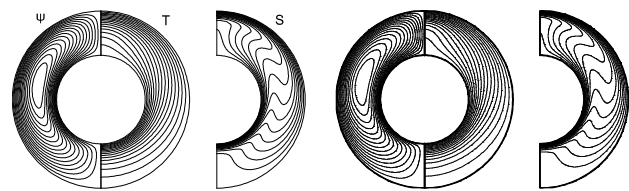
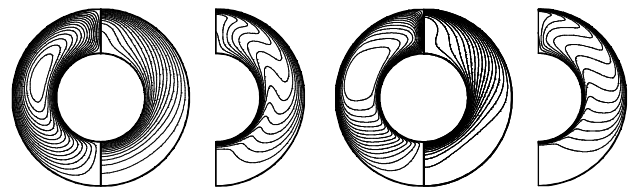


Fig. 8 Evolution of the average Nusselt and Sherwood numbers for different values of  $Le$ , for  $Ra = 50$  and  $N = 1$



(a)  $\psi_{max} = 5.5665$   
 $\overline{Nu} = 1.3429$   $\overline{Sh} = 3.3624$

(b)  $\psi_{max} = 6.5195$   
 $\overline{Nu} = 1.4971$   $\overline{Sh} = 4.0030$



(c)  $\psi_{max} = 7.2476$   
 $\overline{Nu} = 1.6291$   $\overline{Sh} = 4.5426$

(d)  $\psi_{max} = 12.1337$   
 $\overline{Nu} = 2.6557$   $\overline{Sh} = 8.7938$

Fig. 9 Streamlines, isotherms and isoconcentrations for different values of  $N$  for  $Ra = 50$  and  $Le = 5$  (a)  $N = 0$ , (b)  $N = 0.5$ , (c)  $N = 1$ , (d)  $N = 7$

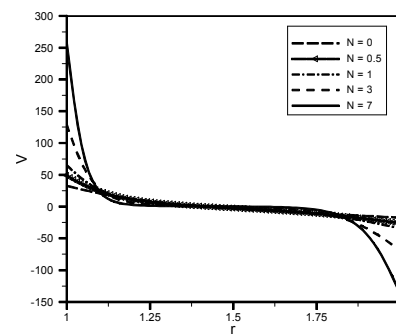


Fig. 10 Tangential component of velocity for  $\phi = \frac{\pi}{2}$  for different values of  $N$ , for  $Ra=50$  and  $Le=5$

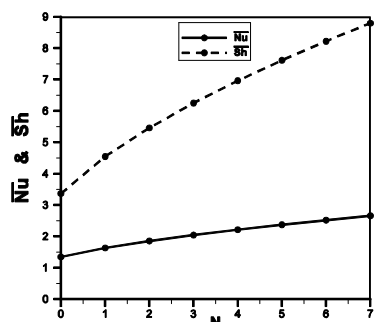


Fig. 11 Evolution of the average Nusselt and Sherwood numbers for different values of  $N$ , for  $Ra = 50$  and  $Le = 5$

#### IV. CONCLUSION

A numerical investigation of double-diffusive natural convection in a horizontal porous annulus saturated with a binary fluid using the ADI method is presented. Results are given for the radius ratio  $R = 2$ . The effect of the control parameters, namely,  $Ra$ ,  $N$  and  $Le$  has been investigated. The variation of these parameters reveals their influence, especially, on the flow structure and on the rates of heat and mass transfer.

#### REFERENCES

- [1] M. Mamou, P. Vasseur and M. Hasnaoui, "On numerical stability analysis of double diffusive convection in confined enclosures," *Journal of Fluid Mechanics*, Vol. 433, pp. 209-250, 2001.
- [2] D. B. Rafael, E. Crespo del Arco, P. Bontoux and J. Ouazzani, "Convection and instabilities in differentially heated inclined shallow rectangular boxes," *C. R. Acad. Sci. Paris*, t. 326, Serie II B, pp. 711-718, 1998.
- [3] D. Gobin and R. Bennacer, "Cooperating thermosolutal convection in enclosures - II. Heat transfer and flow structure," *Int. J. Heat Mass Transfer*, Vol. 39, No. 13, pp. 2683-2697, 1996.
- [4] O. V. Trevisan and A. Bejan, "Natural convection with combined heat and mass transfer buoyancy effects in a porous medium," *Int. J. Heat Mass Transfer*, Vol. 38, No. 8, pp. 1597-1611, 1985.
- [5] F. Alavyon, "On natural convection in vertical porous enclosures due to prescribed fluxes of heat and mass at the vertical boundaries," *Int. J. Heat Mass Transfer*, Vol. 36, No. 10, pp. 2479-2498, 1993.
- [6] M. Hasnaoui, P. Vasseur, E. Bilgen and L. Robillard, "Analytical and numerical study of natural convection heat transfer in a vertical porous annulus," *Chen. Eng. Comm.*, Vol. 136, pp. 77-94, 1995.
- [7] M. Marcoux, M.-C. Charrier-Mojtabi and M. Azaiez, "Double diffusive convection in an annular vertical porous layer," *Int. J. Heat and Mass Transfer*, Vol. 42, pp. 2313-2315, 1999.
- [8] H. Beji, R. Bennacer and R. Duval, "Double-diffusive natural convection in a vertical porous annulus," *Num. Heat Transfer, Part A*, Vol. 36, pp. 153-170, 1999.
- [9] P. W. Shipp, M. Shoukri, and M. B. Carver, "Double diffusive natural convection in a closed annulus," *Num. Heat Transfer*, Vol. 24, pp. 339-356, 1993.
- [10] S. Chen, J. Tolke, and M. Krafczyk, "Numerical investigation of double-diffusive (natural) convection in vertical annuluses with opposing temperature and concentration gradients," *Int. J. Heat Fluid Flow*, Vol. 31, pp. 217-226, 2010.
- [11] J. Belabid and A. Cheddadi, "Comparative Numerical Simulation of Natural Convection in a Porous Horizontal Cylindrical Annulus," *Applied Mechanics and Materials*, Vol. 670 - 671, pp. 613 - 616, 2014.
- [12] F. A. Hamad and M. K. Khan, "Natural Convection Heat Transfer in Horizontal and Inclined Annulus of Different Diameter Ratios," *Energy Convers. Mgmt*, Vol. 39, No. 8, pp. 797-807, 1998.
- [13] H. H. Bau, G. McBlane, and I. Sarferstein, "Numerical simulation of thermal convection in an eccentric annulus containing porous media", *ASME 83 WA/HT 34*, 1983.

- [14] M. C. Charrier-Mojtabi, "Numerical simulation of two- and three dimensional free convection flows in a horizontal porous annulus using a pressure and temperature formulation," *Int. J. Heat Mass Transfer*. Vol. 40, No. 7, pp. 1521-1533, 1997.
- [15] G. Desrayaud, A. Fichera, M. Marcaux, and A. Pagano, "An analytical solution for the stationary behaviour of binary mixtures and pure fluids in a horizontal annular cavity," *Int. J. Heat and Mass Transfer*, Vol. 49, pp. 3253-3263, 2006.
- [16] Z. Alloui, and P. Vasseur, "Natural convection in a horizontal Annular porous cavity saturated by a binary mixture," *Computational Thermal Sciences*, Vol. 3(5), pp. 407-417, 2011.

**Ahmed Ja** Ph.D student in Modeling and Scientific Informatics department with Research Team "Thermal Systems and Real Flows" in Mohammadia School of Engineers, Mohammed V University, Rabat. He holds a Master's degree in "Design, Simulation and Management of Industrial Processes" from National School of Mineral Industry, Rabat. His current research is aimed to study the phenomenon of heat and mass transfers in a saturated porous medium confined in a cylindrical annular geometry.